PRECISION MEASUREMENTS OF β-ENERGY SPECTRA IN NUCLEAR DECAYS: STUDY OF THE SENSITIVITY TO THE DETECTOR CALIBRATION*

X. Huyan, M. Hughes, O. Naviliat-Cuncic

National Superconducting Cyclotron Laboratory
and Department of Physics and Astronomy, Michigan State University
East Lansing MI 48824, United States

(Received December 11, 2017)

A study of the detector calibration sensitivity for measurements of the shape of β-energy spectra is reported using Monte Carlo simulated spectra. An auto-calibration method is proposed which can be carried out simultaneously to the actual measurements. The statistical impact of such a procedure results in a 30% larger uncertainty on the Fierz term compared to a situation in which the detector calibration was exactly known.

DOI:10.5506/APhysPolB.49.249

1. Introduction

Precision measurements of the Fierz interference term in nuclear and neutron decays provide sensitive means to search for exotic scalar and tensor interactions coupling to left-handed neutrinos [1, 2]. The most direct way to access this term is through measurements of the shape of the β-energy spectrum and the current precision goal aims at a sensitivity level below 10^{-3} [2]. A critical aspect in measurements of the shape of β-energy spectra is the detector calibration. This is illustrated in a recent effort in neutron decay [5], which shows how uncertainties in the energy reconstruction or in the linearity of the detector response can preclude the extraction of any useful information on exotic couplings from a spectrum measurement.

The oral presentation reported the status of measurements of β-energy spectra in ^{6}He and ^{20}F decays which were carried out using a calorimetric technique with ions implanted in suitable detectors. A description of the technique can be found elsewhere [3, 4]. Two important instrumental effects

* Presented at the XXXV Mazurian Lakes Conference on Physics, Piaski, Poland, September 3–9, 2017.

were discussed namely, the effect of the detector gain which enters the calibration and a correction due to fast pile-up. This contribution focuses on the first of them and discusses also other properties entering the detector calibration.

The study reported here has been performed using Monte Carlo simulated spectra which were built into histograms assuming a given calibration. The parameters of the calibration were either fixed in the fit function or left as free parameters in order to determine their impact on the physically relevant quantities. The three properties of the calibration that have been studied are: *(i)* the detection system gain; *(ii)* the offset or pedestal; and *(iii)* the non-linearity. The study presented here was made on the energy spectrum of ^{6}He decay.

2. Spectrum shape

For simplicity, the simulated energy spectra have been generated taking the phase-space factor of an allowed transition, $P(W) = pW(W_0 - W)^2$, multiplied by a factor that contains two dynamic terms [6]

$$N(W)\mathrm{d}W = P(W)\left(1 + C_1 W + \frac{m_e}{W} b_{\mathrm{GT}}\right)\mathrm{d}W\,. \tag{1}$$

Such a form is sufficient to illustrate the main aspects associated with the detector calibration. In Eq. (1), W is the total energy of the β particle, p the momentum, W_0 the maximal total energy, m_e the electron mass, C_1 is a coefficient associated with the weak magnetism form factor and b_{GT} is the Fierz interference term. In a Gamow–Teller transition, b_{GT} includes the contribution of tensor-type interactions and is zero within the Standard Model. In ^{6}He decay, the maximal β kinetic energy is $Q = 3.5$ MeV and the value of the coefficient of the linear term can be obtained from the principle of conservation of the vector current and amounts to $C_1 = 0.650(7)\%/\mathrm{MeV}$ [3].

Spectra generated following Eq. (1) were built into histograms by expressing the kinetic energy, E, of the β particle in channels. If the response of the detection chain is linear, the relation between the kinetic energy and the channel value is

$$C(E) = A \cdot E + B\,, \tag{2}$$

where A is the gain of the system and B is the offset or pedestal. It is worth noticing that the units of the channel in Eq. (2) are associated with the digitizing process of a signal corresponding to a kinetic energy E. Those units can be called "Analog to Digital Converter units" or "Digitizer units" or more commonly "channels" (chan), and are to be distinguished from the bins in a histogram. If the bin width of a histogram corresponds to the digitizer resolution then a digitizer unit (or channel) is identical to a bin. To illustrate this more clearly, Fig. 1 shows two histograms obtained from the same generated spectrum over the same interval of channels but with different numbers of bins. The spectrum contains 10^6 events and was obtained by taking the value of the kinetic energy in keV. The values of the parameters in Eq. (2) were $A = 1.7$ chan/keV and $B = 20$ chan. The histogram in the left panel has 4096 bins and in the right panel, 128. This distinction is important when expressing the sensitivities in terms of the units of parameters entering the calibration.

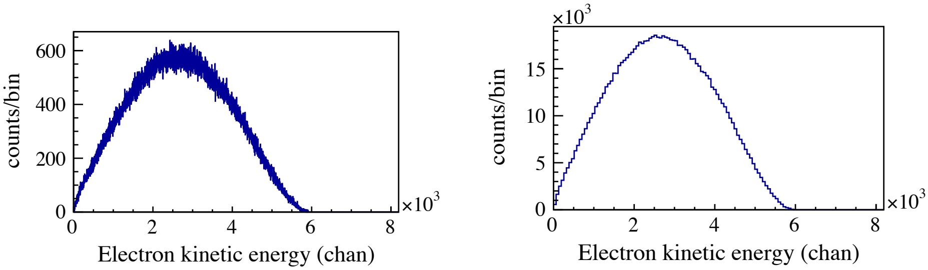

Fig. 1. Simulated β-energy spectrum in ^{6}He decay, with 10^6 events distributed among 4096 bins (left panel) and 128 bins (right panel). The range in digitizer units (or channels) is the same for both histograms. The spectrum was generated including only the phase-space factor.

3. Sensitivity to the detector calibration

The parameter C_1 in Eq. (1) gives rise to a positive slope in the spectrum, whereas b_{GT} gives rise to a negative slope. Calibration effects that would distort the theoretical description of the β spectrum can result in a systematic effect for the extraction of C_1 and b_{GT}. The most sensitive distortion arises from the description of the phase-space factor, $P(W)$.

Figure 2 illustrates how such a systematic effect is produced. The illustration uses here the gain as the parameter to be systematically in error but similar arguments hold when using the offset or the non-linearity of the system. The black/blue curve in the left panel of Fig. 2 is considered to be the experimental spectrum and the grey/red curve is considered to be the theoretical function to be adjusted to the experimental spectrum. To make the effect visible, the grey/red curve was obtained by applying a stretch (*i.e.* a different gain) of 1.1 relative to the black/blue curve, that is a 10% larger gain. The middle panel in Fig. 2 shows the ratio between a similar grey/red curve to the one shown in the left panel and the black/blue curve but with a stretch factor of 1.001 for the grey/red curve. The systematically wrong description of the black/blue curve by the grey/red curve produces a slope which increases toward the end-point energy. The right panel of Fig. 2 shows the values of the derivative of the ratio shown in the middle panel, weighted with the square root of the amplitude of the black/blue curve in the left panel of Fig. 2. Between 1 and 2 MeV, the average value of the slope is about 0.25%/MeV. This is about 40% of the value of C_1 introduced above. This simple picture shows how a 0.1% systematic error on the gain produces a significant slope that can impact the extraction of C_1 or $b_{\rm GT}$.

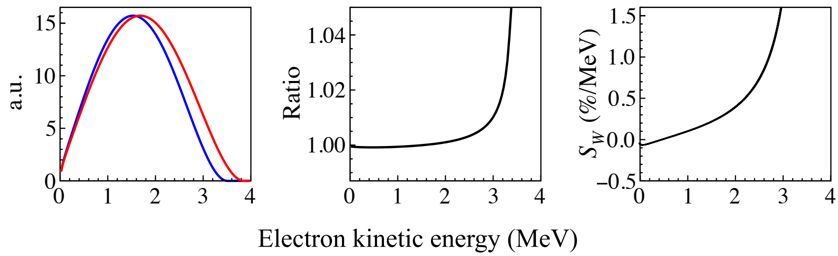

Fig. 2. (Color online) Left panel: analytical β-energy spectrum obtained only from the phase-space factor. The grey/red distribution is obtained from the black/blue distribution by applying a stretch factor of 1.1. Middle panel: ratio between a stretched (grey/red) and an unstretched (black/blue) distribution but with a stretch factor of 1.001. Right panel: slope of the ratio weighted with the square root of the amplitude of the β spectrum distribution.

3.1. General procedure

In order to study the sensitivity of C_1 and $b_{\rm GT}$ to the gain and offset of the calibration, a simple Monte Carlo method has been implemented. A sample of 200 β-energy spectra was generated following Eq. (1) with $C_1 = C_{1\rm MC} = 0.65\%/\rm MeV$ and $b_{\rm GT} = 0$. A linear relation between the energy and the channel was assumed with $A = A_{\rm MC} = 1.5$ chan/keV and $B = B_{\rm MC} = 20$ chan. These values are typical for the experimental conditions described in Ref. [4]. Each spectrum contained 10^6 events distributed over 256 bins. The spectra were fitted using the χ^2 method over a range of channels corresponding to an energy range of 300–3200 keV. Two types of fits were performed, referred below with the labels "SM" and "BSM". In the SM fits, $b_{\rm GT}$ was fixed to 0, and C_1 was left as a free parameter along with the overall normalization. In the BSM fits, C_1 was fixed to 0.65%/MeV and $b_{\rm GT}$ was left as a free parameter along with the normalization.

3.2. Gain

The sensitivity to the gain was studied by fixing the values of the gain in the fit function over the range of 1.495–1.505 chan/keV in steps of 0.001 chan/keV, with the offset fixed to $B = B_{\rm MC}$. For each fixed gain, the average value of C_1 extracted from the SM fits and the average value of

b_{GT} extracted from the BSM fits were calculated. The results are shown in Fig. 3 as a function of the relative gain difference

$$A_{\mathrm{r}} = \frac{A}{A_{\mathrm{MC}}} - 1\,, \tag{3}$$

where A is here the gain fixed in the fit function. From the left panel of Fig. 3, one extracts the sensitivity of C_1 of $-0.29\%/\mathrm{MeV}$ per 0.1% variation of A_{r}. This is comparable to the observations made in Sec. 3.1 with an analytical distribution (Fig. 2). From the right panel of Fig. 3, one extracts the sensitivity of b_{GT} of 1.4% per 0.1% variation of A_{r}.

It is important to point out that it is a variation of the relative gain (or relative gain difference), rather than a variation of the absolute gain, that is relevant to characterize the sensitivities of C_1 and b_{GT}. The same sensitivities are obtained with other absolute values of A_{MC} provided that the range of values of A_{r} remains the same.

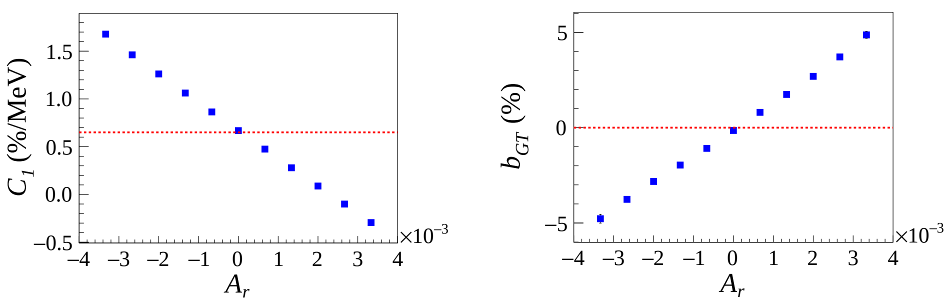

Fig. 3. Average values of C_1 (left panel) and b_{GT} (right panel) obtained from 200 fits as a function of the relative gain difference. The dashed lines indicate the input values of C_1 and b_{GT} used in the simulations.

3.3. Offset

The sensitivity to the offset was studied by fixing the offset in the fit function over the range of 15–25 chan, in steps of 1 chan, with the gain fixed at $A_{\mathrm{MC}} = 1.5$ chan/keV. The average values for C_1 and b_{GT} are shown in Fig. 4 and their sensitivity to the value of B are respectively $-0.1\%/\mathrm{MeV}$ and 0.57% per channel.

It is worth stressing that it is a variation of the absolute value of the offset in channels that is relevant to characterize the sensitivities of C_1 and b_{GT}. A different value of the offset produces the same sensitivity if the variation of the value covers the same range in absolute values.

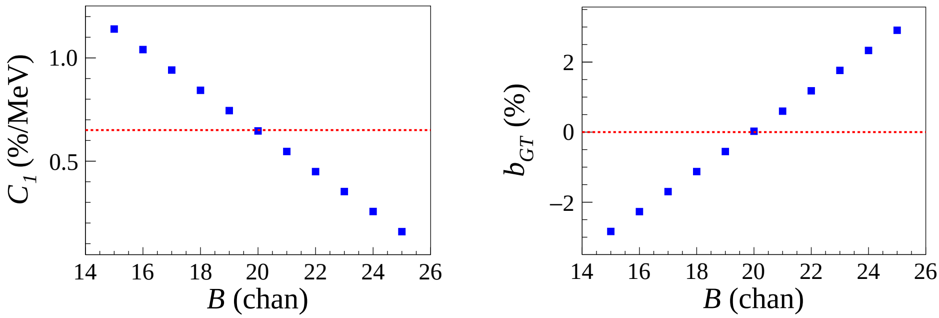

Fig. 4. Average values of C_1 (left panel) and $b_{\rm GT}$ (right panel) obtained from 200 fits as a function of the offset fixed in the fits. The dashed lines indicate the input values of C_1 and $b_{\rm GT}$ used in the simulations.

3.4. Non-linearity

The sensitivity to a non-linear response of the detection chain was studied by following a similar procedure as described in Sec. 3.1 but assuming a quadratic relation between the kinetic energy and the channel number

$$C(E) = aE^2 + bE + c\,. \tag{4}$$

The non-linearity effect can be characterized by a single parameter, P, which describes the deviation from the linear response at the maximum β kinetic energy, Q. By requiring that at zero kinetic energy the channel number equals to the offset, B, and that at an energy of $Q/2$, the deviation from the linear response is reduced by $P/2$, one obtains the expressions of the coefficients in Eq. (4): $a = -AP/Q$, $b = (AQ - BP)/Q$ and $c = B$. From the β-energy spectrum, the channel in the histogram is obtained by a change of variable which includes the derivative $\mathrm{d}W/\mathrm{d}C$

$$N(C) = N(W)\frac{\mathrm{d}W}{\mathrm{d}C}\,. \tag{5}$$

For illustration, Fig. 5 shows a quadratic calibration curve (dotted/red) for $P = 0.10$. The systematic effect due to a non-linear response was studied by generating simulated spectra with the same values of $C_{1\rm MC}$, $b_{\rm GT}$, $A_{\rm MC}$ and $B_{\rm MC}$ as those used above and by fixing the parameter P in the generated spectra over the range of $(1–9)\times10^{-3}$ in steps of 10^{-3}. The fits of the spectra were then performed assuming a linear response and fixing the values of A and B to those used to generate the spectra. The average values of C_1 and $b_{\rm GT}$ extracted from the fits are shown in Fig. 6. The sensitivity of C_1 and $b_{\rm GT}$ with P can, respectively, be described by the slopes of 0.14%/MeV and −0.6% per 0.1% variation of P.

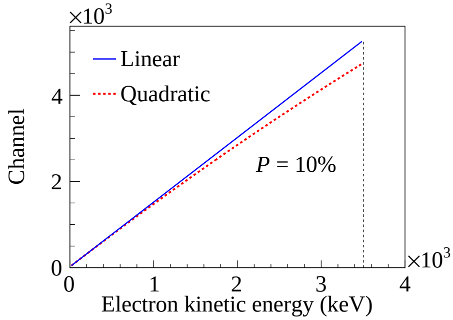

Fig. 5. (Color online) Solid/blue line: linear energy-channel response with $A = 1.5$ chan/keV and $B = 20$ chan. Dotted/red curve: quadratic response with the same values for A and B and with $P = 0.10$.

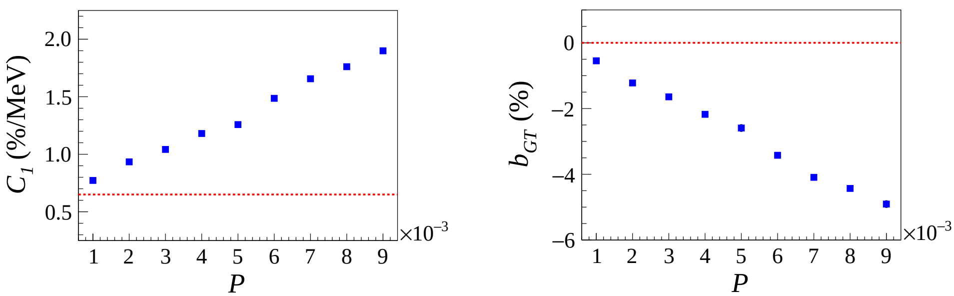

Fig. 6. Average values of C_1 (left panel) and b_{GT} (right panel) obtained from 200 fits as a function of the non-linearity parameter used to generate the simulated spectra. The dashed lines indicate the input values used for the simulated spectra.

3.5. Summary

The sensitivities of C_1 and b_{GT} to variations of the gain, the offset, and the non-linearity coefficient are summarized in Table I. The ranges of values for the three parameters of the calibration have been selected to produce variations of comparable magnitude.

TABLE I

Systematic variations of C_1 and b_{GT} for the corresponding variations of the relative gain difference A_{r}, the offset B and the non-linearity parameter P.

	ΔC_1 [%/MeV]	Δb_{GT} [%]
10^{-3} variation of A_{r}	−0.29	1.4
Unit variation of B (in chan)	−0.1	0.57
10^{-3} variation of P	0.14	−0.6

4. Auto-calibration of the detector gain

The results obtained with the Monte Carlo analysis of Sec. 3 indicate that the detector calibration is extremely critical to reach a precision level of 0.1% on $b_{\rm GT}$. An accuracy smaller than 10^{-4} on the gain is very difficult to reach. Even if this could be achieved in a careful off-line calibration, drifts of the detector gain require to be monitored during the actual measurement, at the same level of accuracy. Furthermore, for the calorimetric technique considered in Ref. [4], it is impossible to probe the same detector volume with external sources as the volume effectively probed by the β particles from ^{6}He decay during their slowing down. These considerations as well as effects related to rate-dependent gain drifts have motivated the implementation of an auto-calibration technique, which is an intrinsic element of the calorimetric method described in Ref. [4]. The auto-calibration technique consists in the determination of an instrumental parameter, here the gain of the detection chain, simultaneously with the relevant physical quantity, either C_1 (or equivalently the weak magnetism form factor) or $b_{\rm GT}$. Such a procedure poses the question of possible correlations between the instrumental parameters and the physical quantities and this is described in this section.

4.1. Fitting spectra with the gain as free parameter

The procedure to study the correlation is similar to that described in Sec. 3.2. A sample of 200 β-energy spectra was generated using the same values of $C_{1\rm MC}$, $b_{\rm GT}$, and $B_{\rm MC}$ as those used in Sec. 3.2. Each spectrum contained 10^6 events in a histogram built over 256 bins. The gain, $A_{\rm MC}$, used to build the histogram was randomly generated in the range of 1.5–1.8 chan/keV. This covers a 20% relative variation of the gain. The spectra were then fitted by a function proportional to Eq. (1). The free parameters in the SM fits were C_1, the gain A, and the overall normalization. For BSM fits, the free parameters were $b_{\rm GT}$, the gain A and the overall normalization. The only difference compared with the fits described in Sec. 3.2 is that the gain was here left as a free parameter.

The gains extracted in the SM fits are shown in Fig. 7. A similar plot is obtained for the BSM fits but the statistical uncertainties are 30% smaller (see below). The upper panel shows the absolute values as a function of the value used in the Monte Carlo to generate the spectra. The lower panel shows the relative gain difference as defined in Eq. (3) but A is here the value of the gain obtained from the fits. It is observed that the values fluctuate more than statistically and this is discussed in Sec. 4.3 below.

Concerning the physics parameters, the left panel of Fig. 8 shows the values of C_1 extracted in the same SM fits as those shown in Fig. 7 and the right panel shows the values of $b_{\rm GT}$ extracted similarly from the BSM fits. The dotted lines indicate the input values used to generate the spectra. The fitted values fluctuate around the input values but do not display any correlation with the absolute value of the gain. This is due to the fact that the dominant term of the fitting function given by Eq. (1), which serves for the calibration, is the phase-space factor.

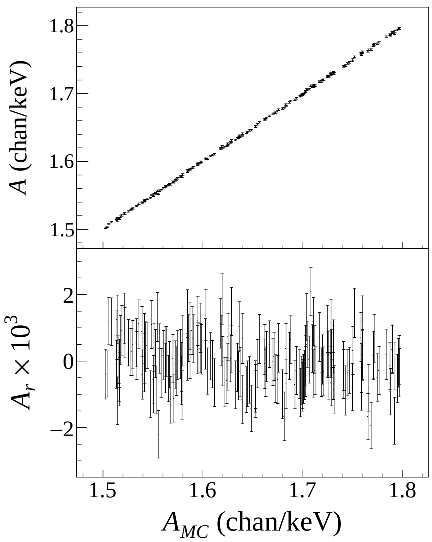

Fig. 7. Absolute value of the gain (upper panel) and relative gain difference multiplied by 1000 (lower panel) obtained in the SM fits as a function of input values of the gain used in the simulations.

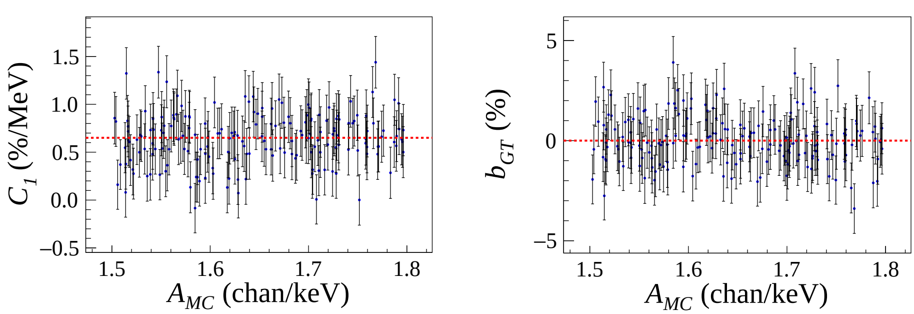

Fig. 8. Values of C_1 (left panel) and $b_{\rm GT}$ (right panel) extracted respectively from the SM and BSM fits when the calibration gain is left as a free parameter. The dotted lines indicate the input values used in the Monte Carlo.

4.2. Statistical uncertainties

Having shown that there is no correlation between the physically relevant parameters and the detector gain, it is interesting to determine the statistical impact of applying this auto-calibration. Figure 9 shows the distributions of the absolute statistical uncertainty on the gain for the SM fits (left panel) and BSM fits (right panel) obtained from a sample of 10^4 spectra. The mean values of the uncertainties are respectively 1.2×10^{-3} chan/keV and 0.9×10^{-3} chan/keV.

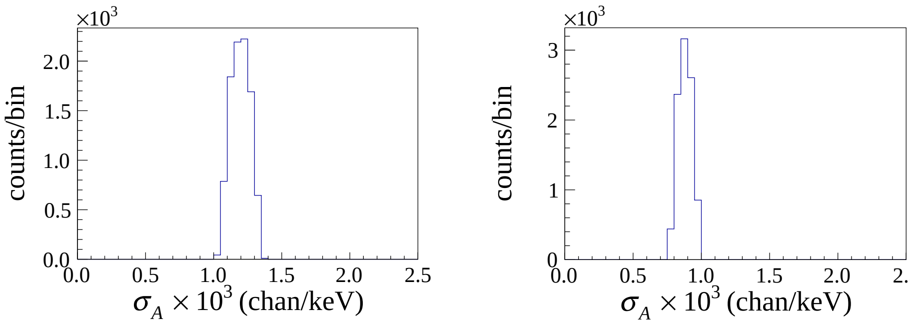

Fig. 9. Distributions of the statistical uncertainties of the gain obtained from the SM fits (left panel) and BSM fits (right panel). The distribution were obtained from a sample with 10^4 simulated spectra.

The distributions of the values of C_1 and $b_{\rm GT}$ extracted from the sample with 10^4 spectra are shown in Fig. 10. The black/blue histogram in the left panel of Fig. 10 corresponds to values of C_1 obtained when the detector gain is left as a free parameter. This corresponds to the distribution of values in the left panel in Fig. 8 but with a larger sample size. The standard

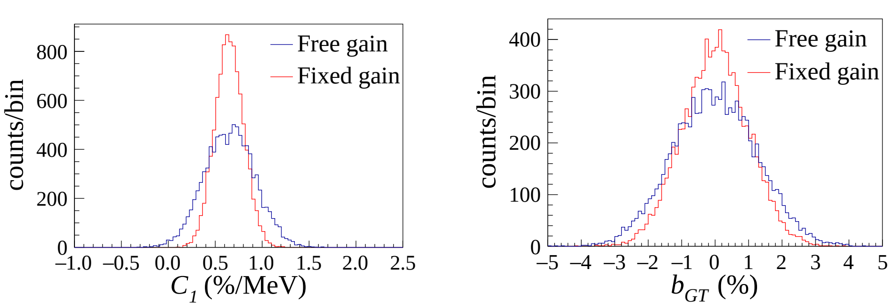

Fig. 10. (Color online) Distributions of values C_1 (left panel) and $b_{\rm GT}$ (right panel) obtained from a sample of 10^4 spectra when the detector gain was left as a free parameter (black/blue distributions) or was considered to be exactly known (grey/red distributions).

deviation of the distribution is 0.27%/MeV. If the detector gain was exactly known, it could then be fixed to the value used to generate the simulated spectra. One obtains then the grey/red histogram in the left panel of Fig. 10 which has a standard deviation of 0.15%/MeV. Leaving the detector gain as a free parameter increases then the statistical uncertainty of C_1 by a factor 1.8. The right panel of Fig. 10 shows similar results for the BSM fits. The standard deviation of the distribution when the gain is a free parameter is 1.25% and would be reduced to 0.98% if the gain was exactly known. As a conclusion, the auto-calibration procedure results in a larger statistical uncertainty on the Fierz term by a factor of 1.28.

4.3. Correlations

The results shown in Fig. 7 and in the left panel of Fig. 8 have been obtained simultaneously in the same fits. An inspection of the fluctuations of individual values shows that, although the values of C_1 are not correlated with the absolute value of the gain, they are, in fact, anti-correlated with the relative difference, $A_{\rm r}$. In analogy to the definition of $A_{\rm r}$, one defines the relative difference on the value of C_1 as

$$C_{1\rm r} = \frac{C_1}{C_{1\rm MC}} - 1, \tag{6}$$

where C_1 is the value obtained from the fits.

The anti-correlation mentioned above is shown in the left panel of Fig. 11, which displays a scatter plot of $C_{1\rm r}$ relative to the relative difference of the gain, $A_{\rm r}$. The right panel in Fig. 11 shows similarly the correlation between the values of $b_{\rm GT}$ and $A_{\rm r}$. These correlations produce the broader distributions shown in Fig. 10.

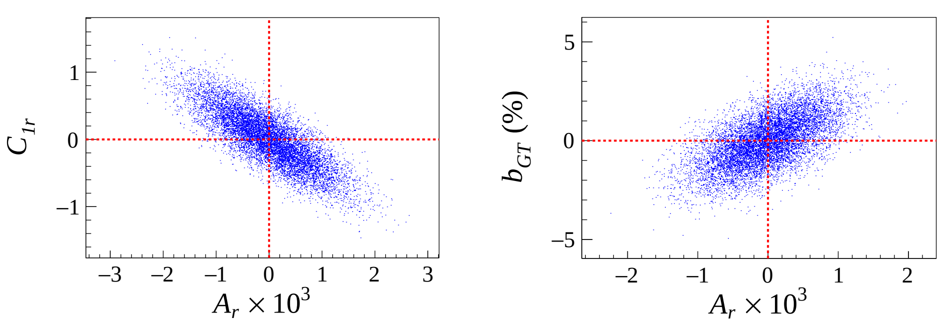

Fig. 11. Left panel: scatter plot of values of C_{1r} *versus* $A_{\rm r}$ from a sample of 10^4 spectra. Right panel: scatter plot of the values of $b_{\rm GT}$ *versus* $A_{\rm r}$.

5. Conclusion

This study described the sensitivity to the detector calibration for the extraction of a linear term and of the Fierz interference term from a precision measurement of the shape of the β-energy spectrum in ^{6}He decay. An alternative auto-calibration method has been proposed which circumvents the needs of an external calibration and provides a direct monitoring of the detector response. The statistical impact of such a method results in a 30% increase on the uncertainty of the Fierz term. This appears to be a moderate compromise with respect to the very challenging task of performing a detector calibration and to monitor its stability at the 10^{-4} level. The present method has been implemented in the data analysis of the experiment in ^{6}He decay [4].

This work has been supported by the U.S. National Science Foundation under grants No. PHY-1102511 and PHY-1565546.

REFERENCES

[1] T. Bhattacharya *et al.*, *Phys. Rev. D* **85**, 054512 (2012).

[2] O. Naviliat-Cuncic, M. González-Alonso, *Ann. Phys. (Berlin)* **525**, 600 (2013).

[3] O. Naviliat-Cuncic, *AIP Conf. Proc.* **1753**, 060001 (2016).

[4] X. Huyan *et al.*, *Hyperfine Interact.* **237**, 93 (2016).

[5] K.P. Hickerson *et al.*, *Phys. Rev. C* **96**, 042501(R) (2017).

[6] L. Hayen *et al.*, `arXiv:1709.07530 [nucl-th]`, accepted for publication in *Rev. Mod. Phys.*